Comparison of 1D debris flow modelling approaches using a high resolution and non-oscillatory numerical scheme based on the finite volume method

C. Rodríguez[1], A. Blanco[2] & R. García[3]
[1]Centro de Investigaciones Aplicadas, CVG-EDELCA, Venezuela
[2]Department of Mechanics, Simón Bolívar University, Venezuela
[3]Department of Civil, Architectural and Environmental Engineering, University of Miami, USA

Abstract

The modelling of debris flow kinematics and mechanics is complex and involves non-linearity at both levels. Until now, the preferred approach in numerical modelling of debris flows is to solve the 1D equations with a Finite Difference method. In order to improve the present debris flow models, we implement a finite volume method stable for Courant numbers up to unity. Mass and Momentum equations are computed using a Roe-type Riemann solver and the MUSCL (Monotone Upwind Schema for Conservation Laws) approach is applied to obtain second order spatial accuracy. Different resistance laws are used for taking account the rheological behaviour of the fluid, considered as a single phase or by a liquid-solid mixture.

The scheme is validated and applied to a debris flow event in Japan. The results show important differences in precision when the proposed model is compared with other numerical models, using the same resistance laws. Results indicate that the Newtonian turbulent Voellmy fluid and Takahashi resistance flow laws better reproduce the front propagation than other rheological models.
Keywords: debris flows, debris flow, finite volume method, resistance laws, rheological behavior of mixtures.

1 Introduction

Debris flow is a common phenomenon in mountain regions. It occurs when masses of poorly sorted sediments agitated and saturated with water surge down slopes in response to gravitational attraction. They are receiving the attention of international community because their occurrence frequency has dramatically increased in recent years. Identification of potential dangerous areas as well as remediation with engineering works are often used to mitigate debris flows effects. Since debris flows are episodic and happen with little warning, it is very important to count on simulation models. Numerical simulations have become an ideal approach for appraising the debris flow propagation.

Most of numerical approaches that have been developed include the use of finites differences [1], finites elements [2] or discrete/distinct element methods [3]. However, the use of models based on finites volume discretization is increasing in computational fluid dynamics due to their conservation properties and precision. Some applications in debris flow based on finite volume have been developed [4].

In this paper a 1D model that takes in account non-linearity is proposed. Shallow water equations, modified for including high slopes are used for expressing conservation of mass and momentum. Rheological behavior of the fluid is considered by using six different constitutive equations. The numerical model is a high resolution and non-oscillatory scheme based on the finite volume method. The scheme is validated for Dam-break problems comparing numerical results with experimental data and applied to a real debris flow event. Comparisons are made between front propagation velocities obtained using different resistances laws and with prediction from the numerical model proposed by Rickenmann and Koch [1].

2 Mathematical model

2.1 Governing equations

The Saint Venant equations for flow in a 1D channel with width variable and rectangular cross section and with bed slope θ are

$$\frac{\partial U}{\partial t} + \frac{\partial F}{\partial x} = S \tag{1}$$

with

$$U = \begin{bmatrix} A \\ AV \end{bmatrix} \tag{2}$$

$$F = \begin{bmatrix} AV \\ V^2 A + ga\bar{y}\cos\theta \end{bmatrix} \tag{3}$$

$$S = \begin{bmatrix} ib \\ F_c + S_0 - S_f \end{bmatrix} \tag{4}$$

where x is the spatial coordinate measured along the length of the channel, t is the time, A(x,t) the area of the flow cross section, V(x,t) the velocity, g the gravity acceleration, $\bar{y}$ the centroid depth of flow area, i the rate of erosion/deposition of the bed, b the width of the channel, S_0 the bed slope (sinθ), S_f the bed resistance term and F_c the pressure force caused by the longitudinal width variations b(x,t) is defined by

$$F_c = \int_0^{h(x,t)} (h - \eta) \frac{\partial b}{\partial x} d\eta \tag{5}$$

with h(x,t) being the mean flow depth.

2.2 Flow resistance laws

Friction term was modeled using different flow resistance laws. Two different cases were considered assuming that the fluid is (a) a homogeneous single phase (Newtonian turbulent and Bingham laminar), (b) a mixture solid-liquid without erosion or deposition of the channel bed (Voellmy and dilatant inertial fluid) or (c) a mixture solid-liquid with erosion or deposition of the channel bed (Egashira model)

2.2.1 Homogeneous single phase models

For a Newtonian turbulent model S_f is obtained from

$$S_f = \frac{n^2 V|V|}{R_h^{4/3}} \tag{6}$$

where *n* is the Manning's roughness coefficient and R_h = A/P is hydraulic radius, P being the wetted perimeter.

For the Bingham plastic model:

$$S_f = \frac{\tau_0}{\rho g h} \tag{7}$$

where τ_0 is the basal shear stress obtained as the solution of the cubic equation

$$2\tau_0^3 - 3\left(\tau_B + 2\frac{\mu_B Q}{h^2}\right)\tau_0^2 + \tau_B^3 = 0 \tag{8}$$

where τ_B is the Bingham yield stress and μ_B the Bingham viscosity.

2.2.2 Solid-liquid mixtures models in non-deformable bed

For a dilatant inertial fluid,

$$S_f = \frac{V|V|}{h^3 \xi^2} \tag{9}$$

where ξ is a parameter accounting for grain and concentration properties in granular flows.

In the case of a Voellmy fluid,

$$S_f = \frac{V|V|}{hC^2} + \cos\theta \tan\delta \tag{10}$$

where C and δ are the Chézy roughness coefficient and the internal friction angle respectively.

2.2.3 Solid-liquid mixtures models in variable form bed

When the bed was let to change, the friction term was modelled following Takahashi approach [5]. Depending on volumetric solid concentration,

$$S_f = \begin{cases} \dfrac{d^2 V|V|}{0.49 g h^2 R_h} & c < 0.2 \\ \dfrac{V|V|}{\left(\dfrac{2}{5d}\dfrac{1}{\lambda}h\right)^2 \dfrac{1}{a_B \sin\delta\left[c + (1-c)\dfrac{\rho_l}{\rho_s}\right] g R_h}} & c > 0.2 \end{cases} \tag{11}$$

where d is the average diameter of solid particles, a_B = 0.042 an empirical constant, c the volumetric solid concentration and being λ expressed by

$$\lambda = \left[\left(\frac{c^*}{c}\right)^{1/3} - 1\right]^{-1} \tag{12}$$

where c* is the bed volumetric solid concentration. Volumetric solid concentration c is obtained as Brufau et al. [4] from

$$\frac{\partial (hc)}{\partial t} + \frac{\partial (hVc)}{\partial x} = i c_v \tag{13}$$

where c_v is given by

$$c_v = \begin{cases} \max\left(c, c_D^*\right) & i \le 0 \\ c^* & i > 0 \end{cases} \tag{14}$$

being c_D^* is the volumetric concentration of deposited material. The rate of erosion/deposition i was obtained using the expression proposed by Egashira and Aschida and described by Brufau et al. [4].

3 Numerical model

The 1D channel reach is defined by N control volumes of equal size Δx. The time increment is Δt. By using the mean value theorem and the divergence theorem, the governing equations represented by eqn (1) can be integrated in each control volume to get:

$$\boldsymbol{U}_j^{k+1} = \boldsymbol{U}_j^k - \frac{\Delta \boldsymbol{t}}{\Delta \boldsymbol{x}}\left(\boldsymbol{F}_R - \boldsymbol{F}_L\right) + \Delta \boldsymbol{t}.\boldsymbol{S} \tag{15}$$

where F_R and F_L are the numerical flows in the right and left boundary of each volume of control and k+1 and k represent time levels $t+\Delta t$ and t respectively. Second order time integration is obtained using the predictor-corrector method as proposed by Sanders [6].

3.1 Predictor step

In the predictor step areas and velocities are approximated by

$$A_j^{k+1/2} = A_j^k - \frac{\Delta t}{2\Delta x}\left(V\Delta A + A\Delta V\right)_j^k \tag{16}$$

$$\begin{aligned} V_j^{k+1/2} = {} & V_j^k - \frac{\Delta t}{2\Delta x}\left(g\Delta h + V\Delta V\right)_j^k \\ & + \frac{g\Delta t}{2}\left[\left(S_0\right)_j^k - \frac{1}{2}\left(S_f\right)_j^k - \frac{1}{2}\left(S_f\right)_j^{k+1/2}\right] \end{aligned} \tag{17}$$

The gradients are limited and prevent oscillations in the solutions witch are very common in second order accurate schemes. For depth and velocity, gradients are estimated through an average function obtained using the superbee limiter [6]. Depth is extrapolated to the cell center where areas are computed. S_0 is given by

$\sin\theta_j$ while that S_f is obtained from eqns. (6-7,9-11). Since that S_f is estimated at the level k+1/2, a semi-implicit formulation is obtained for estimating velocity from Eq. (11). In the case of Newtonian turbulent model eqn. (17) is write as

$$V_j^{k+1/2} = V_j^k - \frac{\Delta t}{2\Delta x}\left(g\Delta h + V\Delta V\right)_j^k + \frac{g\Delta t}{2}\left[\left(S_0\right)_j^k - \frac{1}{2}\left(S_f\right)_j^k - \frac{1}{2}\left(\frac{n^2 V_j \left|V\right|_j}{R_h^{4/3}}\right)_j^{k+1/2}\right] \tag{18}$$

Therefore, velocity is estimated solving a second degree algebraic equation (Rodríguez [7]). The same scheme is used for the others resistance laws less the Bingham model in which the coupled equation system defined by eqn (7) and eqn (8) is expressed in each cell and solved for τ_{0j} and V_j. This is done using Newton-Raphson iterative technique (Rodríguez [7]).

3.2 MUSCL extrapolation

For extrapolation of velocity and depth to the left and right faces of the control volume, at time level k+1/2 MUSCL approximation is used. So, h and V are extrapolated and areas in each face of volume of control are estimated from the area function evaluated at each face.

3.3 Corrector step

In the corrector step, areas and velocities are estimated using eqn (2) and the expression

$$\boldsymbol{U}_j^{k+1} = \boldsymbol{U}_j^k - \frac{\Delta \boldsymbol{t}}{\Delta \boldsymbol{x}}\left(\boldsymbol{F}_{j+1/2}^{k+1/2} - \boldsymbol{F}_{j-1/2}^{k+1/2}\right) + \Delta \boldsymbol{t}.\left(\boldsymbol{S}_F\right)_j^{k+1/2} + \frac{\Delta \boldsymbol{t}}{2}\left[\left(\boldsymbol{S}_S\right)_j^k + \left(\boldsymbol{S}_S\right)_j^{k+1}\right] \tag{19}$$

where numerical fluxes are computed at the faces of each volume of control. Numerical fluxes are evaluated by

$$F_l = \frac{1}{2}\left(F_L + F_R - \left|\hat{A}_U\right|\Delta U\right) \tag{20}$$

where the correction term is evaluated using the matrix $\left|\hat{A}_U\right|$ (Rodríguez [7])

$$\left|\hat{\boldsymbol{A}}_U\right| = \hat{\boldsymbol{R}}\left|\hat{\Lambda}\right|\hat{\boldsymbol{L}} = \frac{1}{2\hat{\boldsymbol{a}}}\begin{pmatrix} 1 & 1 \\ \hat{\boldsymbol{V}}-\hat{\boldsymbol{a}} & \hat{\boldsymbol{V}}+\hat{\boldsymbol{a}} \end{pmatrix}\begin{pmatrix} \hat{\boldsymbol{V}}-\hat{\boldsymbol{a}} & 0 \\ 0 & \hat{\boldsymbol{V}}+\hat{\boldsymbol{a}} \end{pmatrix}\begin{pmatrix} \hat{\boldsymbol{V}}+\hat{\boldsymbol{a}} & -1 \\ -\hat{\boldsymbol{V}}+\hat{\boldsymbol{a}} & 1 \end{pmatrix} \tag{21}$$

Quantities $\hat{V}$ and $\hat{a}$ (wave celerity) are averaged in ROE sense and are computed following Brufau et al. [4]. Source terms are estimated in the same way as in the predictor step.

3.4 Boundary conditions

Ghost cells are defined at inlet and outlet of flow domain. For inlet boundary condition and subcritical flow, velocity is specified, area is extrapolated in first order using adjacent cell values and depth is calculated from area-depth relationship. Depth gradient is extrapolated to first order using adjacent cell values and velocity gradient is zero. For supercritical flow velocity and area are specified and both gradients are zero.

Velocity and area are extrapolated to first order at the outlet using adjacent cell values and gradients are zero for both supercritical and subcritical flow. If area is specified at the outlet, velocity is extrapolated to first order from adjacent cell values.

3.5 Stability conditions

Since the scheme described above is designed for unsteady situations, the time step must be specified to advance the solution. The use of Courant-Friedrichs-Lewy (CFL) criterion is an effective way of choosing an appropriate time step. For cases analyzed here C values were between 0.1 and 0.8.

3.6 Model verification

The model was applied to various problems in order to validate it. Classical dam-break non-friction solutions as Ritter's solution and flow over triangular cross-section channel were reproduced for a channel with a dam at the middle. Simulations were conducted assuming a small fluid layer downstream of the dam position. Results proved to be non-dependent of the layer depth assumed. Also, friction cases were analyzed. In particular comparison with classical WES experiments was done obtaining good agreement. Details can be found in Rodríguez [7]. It is observed that the proposed model is able to reproduce both analytical and experimental flows.

4 Numerical results

Comparison between model simulations and field observations are made for a debris flow event in the Kamikamihori valley in Japan reported by Rickenmann and Koch [1]. Longitudinal profiles and channel width are presented in Fig. 1.

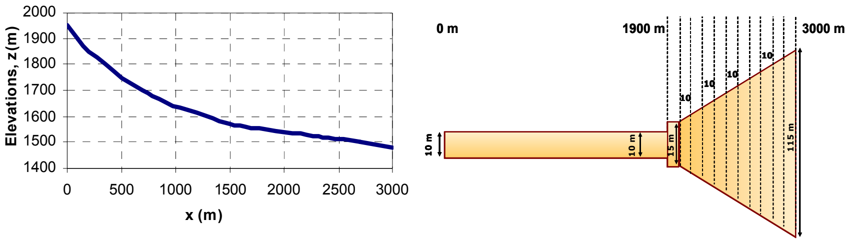

Figure 1: Longitudinal profile and channel width of field case: Kamikamihori valley.

The model channel has a constant width of 10m down to the fan apex at x = 1.9 km. From this point it widens to a width of 15 m, at x = 2.0 km and further downstream there is a widening of 10 m per 100 m of longitudinal distance. The input hydrograph at x = 0 km has a maximum flow depth of 2.5 m, a constant inflow velocity of 6.5 m/s during 40 s. The total volume hydrograph (water and sediment) correspond to 6500 m^3. After 40 s, input velocity is set to zero.

Numerical parameters were as follow. A reach with 2000 cells was built. $\Delta x = 1.5$ and Courant number C was fixed to 0.2. Rheological model parameters were adjusted in order to best reproduce the measured data on flow front velocity along the flow path. As in Rickenmann and Koch [1] an uncertainty margin of 20% was assumed with regard to the measured velocities.

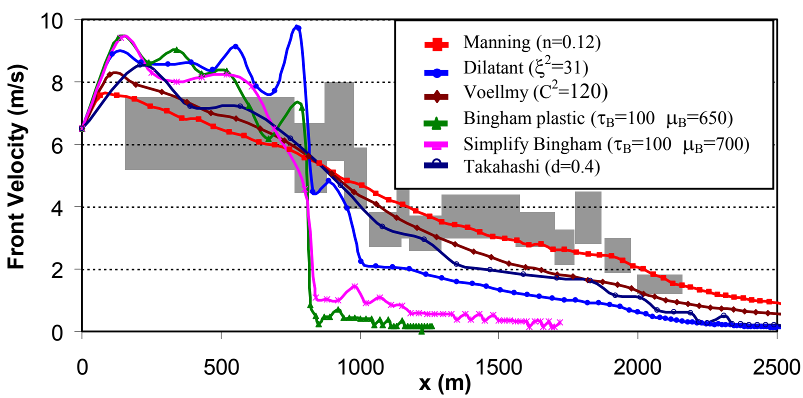

Figure 2: Comparison between observed and simulated velocities in real events.

It can be observed from Fig. 2 that front velocities are reasonably close to the observed ones for the turbulent, Voellmy and Takahashi models. When channel slope change (around 800 m from the starting point) Bingham model predicts front velocities lower than observed. Predictions from dilatant inertial model are far form observed velocities.

However, as is show in fig. 3a, predictions for this rheological model are very much closer to observed velocities using volume finite scheme that those predicted using the lagrangian central finite difference scheme used by Rickenmann and Koch [1]. In particular, Rickenmann and Koch model predict artificially high velocities at the beginning of motion. Similar results are obtained when resistance laws from Bingham plastic model is used (fig. 3b). The proposed model predicts velocities better than Rickenmann and Koch model, showing less dispersion with regard to observed velocities. In addition, Manning coefficient required by our model (0.12) is lower than is required by Rickenmann and Koch model (0.15) that is in agreement with field experience.

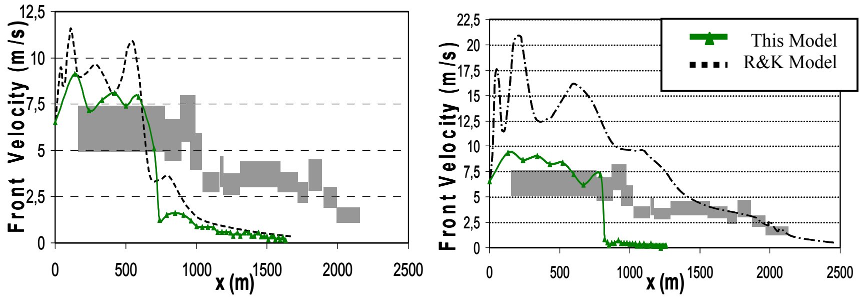

Figure 3: Comparison between predicted velocities using this model and Rickenmman and Koch model (a) dilatant inertial ($\xi^2 = 31\ m^{-1/2}\ s^{-1}$), (b) Bingham plastic ($\tau_B = 100$ Pa $\mu_B = 800$ Pa s).

Since that the numerical nature of each model is different, these results indicate that it is very important to use numerical models with high precision. When non-linearity at motion equations and rheological models are present, precision of numerical solutions could be too low and predictions could be very far from actual values.

5 Conclusions

In this paper a numerical model that solves the 1D shallow water equations modified for including high slopes was developed. The model is based on the finite volume method and can consider constitutive equations for Newtonian turbulent or Bingham plastic fluids.

This model proves to be robust and does not present oscillations often found in second order methods. It was validated and was able to reproduce, analytical solutions and experimental data with very good precision. Numerical instabilities that appear when Bingham plastic rheological model is used were removed introducing a laminar bi-viscous model.

When applied to a real event, better results were obtained with Newtonian turbulent model, Voellmy and Takahashi model. Other constitutive equations should be tested and extension to two-dimensional models should be done in order to achieve substantial progress.

When it is compared with Rickenmann and Koch model, using the same constitutive equations, both models show same trends but the proposed model get best results. It is indicative of the importance of use a robust numerical model to solve motion equations when non-lineal rheological models are employed.

Acknowledgements

This work has been partially financed by the project DI-CAI-012-04 of the Decanato de Investigación y Desarrollo of the University Simón Bolívar (USB), by the project No.G-200001528 of the FONACIT and by the project MILENIO to whom the authors wish to express their appreciation.

References

[1] Rickenmann, D., & Koch, T., *Proc. of first Int. Conf. on Debris-Flow Hazards Mitigation: Mechanics, Prediction, and Assessment*, ed. C. Chen, ASCE, New York, pp. 576-585, 1997.

[2] Frenette, R., Eyheramendy, D. & Zimmermann, T. Numerical modelling of dam-break type problems for Navier-Stokes and granular flows. *Proc. of first Int. Conf. on Debris-Flow Hazards Mitigation: Mechanics, Prediction, and Assessment*, ed. C. Chen, ASCE, New York, pp. 586-595, 1997.

[3] Asmar, B. N., Lanston, P. A. & Ergenzinger, P. The potential of the discrete element method to simulate debris flow. *Proc. of third Int. Conf. on Debris-Flow Hazards Mitigation: Mechanics, Prediction, and Assessment*, eds. D. Rickenmann & C. Chen, MillPress, Rotterdam, pp. 435-445, 2003.

[4] Brufau, P., Garcia-Navarro, P., Ghilardi, P., Natalie, L. & Savi, F., 1D Mathematical Modelling of Debris Flow, *Journal of Hydraulic Engineering*, **38(6)**, pp. 435-446, 2001.

[5] Takahashi T., *Debris Flow*, Balkema, Rotterdam, 1991.

[6] Sanders, B. High-resolution and non-oscillatory solutions of the St. Venant equations in non-rectangular and non-prismatic channels, *Journal of Hydraulic Research*, **39(3)**, pp. 321-330, 2001.

[7] Rodriguez, C. Modelaje numérico de aludes torrenciales utilizando el método de los volúmenes finitos. MSc thesis, Universidad Simón Bolívar, Venezuela, 2006.

[8] WES (Waterways Experiment Station). Floods resulting from suddenly breached dams, Misc paper No. 2-374, Report No 1: Conditions of minimum resistance, 1960, Report No 2: Conditions of high resistance, US Army Corp of Engineers, 1961.